Differential effects of bone structural and material properties on bone competence in C57BL/6 and C3H/He inbred strains of mice

Voide, Romain ; van Lenthe, G Harry ; Müller, Ralph

Abstract: The femoral neck is a relevant and sensitive site for studying the degree of osteopenia. Engineering principles predict that bone structural parameters, like cross-sectional geometry, are important determinants of bone mechanical parameters. Mechanical parameters are also directly affected by the material properties of the bone tissue. However, the relative importance of structural and material properties is still unknown. The aim of this study was to compare bone competence and structural parameters between a murine strain showing a low bone mass phenotype, C57BL/6 (B6), and another one showing a high bone mass phenotype, C3H/He (C3H), in order to better determine the role of bone structure and geometry in bone failure behavior. Murine femora of 12- and 16-week-old B6 and 12- and 16-week-old C3H inbred strains were mechanically tested under axial loading of the femoral head. In order to assess the structural properties, we performed three-dimensional morphometric analyses in five different compartments of the mouse femur using micro-computed tomography. The mechanical tests revealed that B6 femora became stiffer, stronger, and tougher at 12-16weeks, while bone brittleness stayed constant. C3H bone stiffness increased, but strength remained constant, work to failure decreased, and bone became more brittle. These age effects indicated that B6 did not reach peak bone properties at 16weeks of age and C3H did reach maximal skeletal biomechanical properties before 16weeks of age. Our investigations showed that 83% of the strength of the femoral neck in the B6 strain was explained by cortical thickness at this location; in contrast, in C3H none of the mechanical properties of the femoral neck was explained by bone structural parameters. The relative contributions of bone structural and material properties on bone strength are different in B6 and C3H. We hypothesize that these different contributions are related to differences at the ultrastructural level of bone that affect bone failure

DOI: https://doi.org/10.1007/s00223-008-9120-y

Calcif Tissue Int (2008) 83:61–69
DOI 10.1007/s00223-008-9120-y

LABORATORY INVESTIGATIONS

Differential Effects of Bone Structural and Material Properties on Bone Competence in C57BL/6 and C3H/He Inbred Strains of Mice

Romain Voide · G. Harry van Lenthe · Ralph Müller

Received: 21 September 2007 / Accepted: 3 March 2008 / Published online: 11 June 2008

Abstract The femoral neck is a relevant and sensitive site for studying the degree of osteopenia. Engineering principles predict that bone structural parameters, like cross-sectional geometry, are important determinants of bone mechanical parameters. Mechanical parameters are also directly affected by the material properties of the bone tissue. However, the relative importance of structural and material properties is still unknown. The aim of this study was to compare bone competence and structural parameters between a murine strain showing a low bone mass phenotype, C57BL/6 (B6), and another one showing a high bone mass phenotype, C3H/He (C3H), in order to better determine the role of bone structure and geometry in bone failure behavior. Murine femora of 12- and 16-week-old B6 and 12- and 16-week-old C3H inbred strains were mechanically tested under axial loading of the femoral head. In order to assess the structural properties, we performed three-dimensional morphometric analyses in five different compartments of the mouse femur using micro-computed tomography. The mechanical tests revealed that B6 femora became stiffer, stronger, and tougher at 12–16 weeks, while bone brittleness stayed constant. C3H bone stiffness increased, but strength remained constant, work to failure decreased, and bone became more brittle. These age effects indicated that B6 did not reach peak bone properties at 16 weeks of age and C3H did reach maximal skeletal biomechanical properties before 16 weeks of age. Our investigations showed that 83% of the strength of the femoral neck in the B6 strain was explained by cortical thickness at this location; in contrast, in C3H none of the mechanical properties of the femoral neck was explained by bone structural parameters. The relative contributions of bone structural and material properties on bone strength are different in B6 and C3H. We hypothesize that these different contributions are related to differences at the ultrastructural level of bone that affect bone failure.

Keywords Inbred strain · Biomechanics · Bone strength · Bone structure · Bone quality

R. Voide · G. H. van Lenthe · R. Müller
Institute for Biomedical Engineering, University and ETH Zürich, Moussonstrasse 18, 8044 Zurich, Switzerland

R. Voide
e-mail: voider@ethz.ch

G. H. van Lenthe
e-mail: vanlenthe@ethz.ch

R. Müller (✉)
Institute for Biomechanics, ETH Zürich,
Wolfgang-Pauli-Strasse 10, 8093 Zurich, Switzerland
e-mail: ram@ethz.ch
URL: http://www.biomech.ethz.ch

The primary cause of hip fracture is osteoporosis, a disease that reduces bone density below the level needed for mechanical support of normal activities [1]. Attempts at identifying individuals at risk of hip fracture have involved identifying those with critically reduced levels of bone density. The procedure requires that the clinician obtain a dual-energy X-ray absorptiometric (DXA) scan of the patient's proximal femur. Bone mineral density (BMD) is measured at various regions of interest and compared with the mean femoral BMD of a healthy population (chosen as the reference level). However, the two density distributions, of patients at-risk and age-matched controls, have been found to overlap by large amounts, reducing the accuracy of

classification to about 65% [2]. It has been shown that, in addition to BMD, other structural parameters, such as bone architecture and bone geometry, also play a nonnegligible role in determining bone competence [3–8].

The use of the mouse as a model for human musculoskeletal diseases has increased in popularity as the mouse genome has been well characterized. The advantages of the mouse model are that various strains have been observed to exhibit disease state characteristics similar to those found in humans and that the mouse is easily accessible to manipulation of the genetic makeup by either gene knockout, gene overexpression (transgenes), or genetic breeding strategies [9]. With the exception of identical twins, the genetic background in humans varies significantly from one individual to another, making studies of genetic involvement in a given bone phenotype in humans difficult. Well-characterized animal lines, such as murine inbred strains, with phenotypes related to certain aspects of human osteoporosis are therefore used as an approach to study more homogeneous populations.

Previous studies on rabbit, rat, and mouse bones evaluated femoral neck strength [10–15]. In these studies, femora were loaded at the femoral head in a direction parallel to the femoral shaft axis. The loading configuration is not physiological since the effect of musculature is neglected and the morphology of mouse femora differs from that of human femora. Nevertheless, it has been used so far in order to investigate bone mechanical and material properties in the sensitive site of the femoral neck.

Despite the wide variety of clinical methods available today for assessing bone properties, nondestructive imaging methods such as peripheral quantitative computed tomography (pQCT) and DXA have limited use for evaluation of microstructural parameters due to the small size of murine bones. Histomorphometry, despite its very high resolution, is a destructive and time-consuming method. Alternatively, micro-computed tomography (μCT) is fully nondestructive and well-suited for assessing truly three-dimensional (3D) microstructural bone properties [16–21]. Previous studies have shown μCT to be an accurate technique, with close correlations between microtomographic and histomorphometric measurements of static structural bone metrics in various applications [22–26].

Adult C3H/HeJ (C3H) and C57BL/6J (B6) mice are similar in body size and weight, and their bones are of similar external size but show significantly different morphological traits [27–29], such as adult peak bone density and bone cross-sectional area [30, 31]. More importantly, these two strains have often been identified as a model system for high (HBM, C3H) and low (LBM, B6) bone mass phenotypes [32, 33] to study genetic factors in osteoporosis. In the present study, we evaluated the microstructural and mechanical properties in the femoral neck of the two inbred strains B6 and C3H. We hypothesized that microstructural properties would predict mechanical behavior of the femoral neck differently in the two mouse strains. Therefore, our aim was to compare femoral neck competence and morphometric parameters of the two strains in order to better determine the role of bone structure and geometry in the process of bone failure at this precise location. For this purpose, murine femoral heads were loaded in the axial direction and a compartmental morphometric analysis of the femoral diaphysis, metaphysis, and neck was performed. As far as we know, there have been no earlier attempts to evaluate the morphometric properties of the femoral neck compartment by means of μCT.

Materials and Methods

Animal Model

For this study, we used two inbred strains, where B6 represented the LBM and C3H the HBM phenotype. All mice were female and raised at Harlan (Horst, The Netherlands). They were killed by CO_2 inhalation at 12 or 16 weeks. The animals were then stored at –20°C and thawed at room temperature just before dissection of the femora. Eight femora from 12-week-old B6, eight femora from 16-week-old B6, 20 femora from 12-week old C3H, and 12 femora from 16-week-old C3H were dissected. Use of mice in this research project was reviewed and approved by the local authorities for all levels of investigation.

Morphometric Analysis

After removing soft tissue, each bone was measured using desktop μCT (μCT 40; Scanco Medical, Bassersdorf, Switzerland) equipped with a 5 μm focal spot X-ray tube as a source. A 2D charge-coupled device, coupled to a thin scintillator as a detector, permitted acquisition of 20 tomographic images in parallel. The long axis of the femur was orientated orthogonal to the axis of the X-ray beam [34]. The X-ray tube was operated at 50 kVp and 160 μA. The integration time was set to 100 milliseconds. Scans were performed at a nominal resolution of 20 μm in all three spatial dimensions (medium resolution mode). This resolution is high enough to measure with high accuracy the trabecular and cortical morphometric parameters [34]. 2D CT images were reconstructed in 1,024 x 1,024 pixel matrices from 1,000 projections using a standard convolution-backprojection procedure with a Shepp and Logan filter. Images were stored in 3D arrays with an isotropic voxel size of 20 μm. Then, they were rotated in a standard orientation and a constrained 3D gaussian filter was used to suppress partly the noise in the volumes ($\sigma = 1.2$ and support $= 1$).

Morphometric analyses were performed in five different compartments. Compartment I included the full femur, compartment II contained the trabecular bone in the distal metaphysis, and compartment III comprised a 1-mm-thick slab in the midshaft. These three compartments were determined, generated, and analyzed in the same way as described earlier [34]. For the purposes of this study, two new compartments were defined: compartment IV comprised the cortical bone of the femoral neck, and compartment V included the trabecular bone of the femoral neck. These new compartments were generated fully automatically using IPL scripts (Scanco Medical) based on distance transformation (DT) [35] and on classical erosion and dilation algorithms. Since the femoral neck is thinner than the femoral head and the femoral diaphysis, it was defined as the region between the head and the diaphysis with thickness below a fixed threshold value. We developed an algorithm that first measured the thickness of the full bone, as previously described [35]. Then, all the structures below a certain thickness were isolated. In most cases, this procedure isolated the neck, but sometimes also the third trochanter and one condyle accompanied the neck. A component labeling algorithm was applied to select the neck only. The threshold value was determined relative to the average cortical bone thickness of the full femur compartment. This new type of adaptive mask permitted isolation of the neck region in a straightforward and reproducible way, independently of the geometric differences between the individual samples (Fig. 1).

In order to separate compartments IV (neck cortical bone) and V (neck cortical bone), cortical and trabecular bone were distinguished by successive erosion and dilation steps.

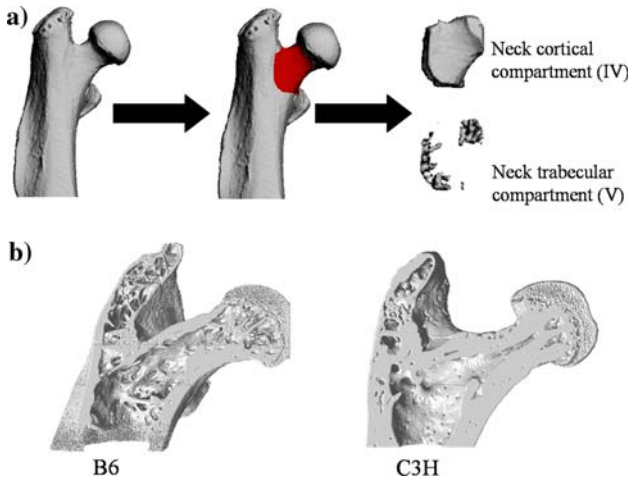

Fig. 1 (**a**) μCT images of each femur were used to automatically isolate the femoral neck for morphological analysis. *Right* Compartment IV, femoral neck cortical bone; compartment V, femoral neck trabecular bone. (**b**) Differences in cross-sectional geometries of the proximal femur between B6 and C3H are clearly visible. B6 shows more trabecular structures, while cortical bone in C3H is thicker

For segmentation, the threshold values were set to 22.4% of the maximum gray-scale value, as previously described [36], for the full femur, diaphysis cortical, and cortical neck compartments and to 16.0% for the diaphyseal trabecular and trabecular neck compartments.

Morphometric traits were determined using a direct 3D approach [37] in each of the five different analysis compartments. For the whole bone, only apparent volume density (AVD) was assessed, which is the number of bone voxels, defined by the thresholding procedure, divided by the number of all voxels within the outer contour describing the bone envelope. Parameters determined in the metaphyseal trabecular and neck trabecular bone included bone volume density (BV/TV), trabecular thickness (Tb.Th), trabecular spacing (Tb.Sp), trabecular number (Tb.N), and connectivity density (Conn.D). Seven geometric parameters, including total volume (TV), cortical bone volume (Ct.V), bone surface area (BS), bone volume density (Ct.V/TV), bone surface density (BS/TV), bone surface to volume ratio (BS/BV), and cortical average thickness (Ct.Th) were assessed in the 1-mm-thick cortical volume in the diaphysis and in the femoral neck cortical bone. Cortical bone thickness was measured using the thickness algorithm developed by Hildebrand and Rüegsegger [35]. Two further parameters were computed in the diaphyseal cortical compartment: anterior-posterior diameter (APD) and average cross-sectional area (T.Ar).

Biomechanical Testing

For testing, the femora were cut above the condyles, resulting in a length of 11 ± 0.5 mm. After rigorous alignment of the samples, which ensured an axial reproducibility error of only 1.5° [38], the femora were embedded with cyanoacrylate glue (Superglue; UHU Schweiz, Schönenwerd, Switzerland) into aluminum bone holders, which could then be rigidly fixed in the testing device. Compressive loading was applied at the femoral head in a custom-made loading device, which was integrated in a materials testing machine (1456; Zwick, Ulm, Germany) (Fig. 2). Load-displacement curves were recorded at a crosshead speed of 0.5 mm/second [29]. From these curves, bone strength (maximum force), stiffness (slope of the linear part of the curve), brittleness (deformation to failure; the smaller the deformation is, the more brittle the sample is), and work to failure were assessed (Fig. 3).

Statistical Analysis

Both strain and age groups were compared at the mechanical and morphometric levels using one-way

Fig. 2 A left femur of a C3H mouse positioned in the materials testing machine and loaded axially

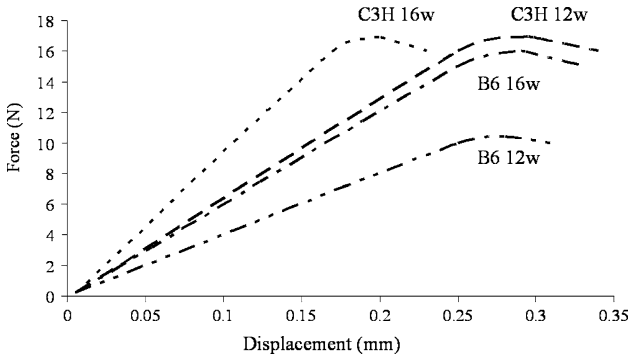

Fig. 3 Average load–displacement curves of the four groups

analysis of variance (ANOVA) with a least significant difference (LSD) post hoc analysis, where the significance level was set to $P < 0.05$. Relationships between mechanical and morphometric parameters were computed using single and multiple linear regression analyses. All statistical analyses were performed with MS Excel 2003 (Microsoft, Redmond, WA), the GNU statistical package R (version 2.4.0, http://www.r-project.org), and the statistical program SPSS (version 13.0; Apache Software Foundation, Chicago, IL).

Results

In B6, all the mechanical values, except failure deformation, increased significantly with age ($P < 0.01$) (Table 1). Femora became stronger, stiffer, and tougher; but bone brittleness did not change. The C3H strain behaved differently. Stiffness and brittleness significantly increased ($P < 0.01$). Strength remained constant, and work to failure decreased ($P < 0.01$) (Table 1).

Linear regression analyses between the mechanical parameters and the morphometric indices of the five compartments were performed. In B6, strength was best explained by Ct.V/TV (67%, $P < 0.001$) and Ct.Th (83%, $P < 0.001$) as measured in the neck compartment (Fig. 4). The other mechanical parameters from B6 were not predicted by any morphometric parameter of any compartment. Similar analyses for the C3H strain demonstrated that morphometry did not significantly predict any mechanical parameter. Linear regression showed regressions of $R^2 < 0.5$ in each case. Particularly, the morphometric indices that were good indicators of femoral neck strength in B6, bone volume density, and cortical thickness of the femoral neck cortical compartment influenced bone strength in C3H only very weakly ($R^2 < 0.15$) (Fig. 5).

Correspondences in morphometric indices between the different compartments were also investigated in each strain. Very high correlations between indices of compartments I (full femur), III (midshaft cortical bone), and IV (neck cortical bone) were found in B6. Bone volume density of cortical bone in the femoral neck correlated very well with the apparent bone density of the full bone and with the bone volume density of the diaphysis cortical bone (Fig. 6a, b). Similarly, cortical thickness of the femoral neck correlated significantly with cortical thickness of the diaphysis (Fig. 6c). Since full-bone AVD, diaphyseal Ct.V/TV, and Ct.Th correlated well with neck cortical properties in B6, they were also good predictors of bone strength in B6 ($0.78 < R^2 < 0.82$). In C3H, the geometry of the femoral neck compartment did not correlate significantly with the morphometric indices of any other compartment.

There was almost no trabecular bone in the C3H femoral neck. The few trabeculae that were included in the analyses were too sparse and disconnected to perform a relevant analysis of their contribution to femoral neck mechanics. In B6, the compartmental analysis (compartment V, neck trabecular bone) revealed more trabecular bone, but it showed no contribution to mechanical properties. Thus, because of the absence of trabecular bone in one strain and the lack of correlation between cortical bone morphometry and neck mechanics in the other one, trabecular bone properties were not reported.

Table 1 Neck morphometric and mechanical results

	B6		C3H	
	12 weeks	16 weeks	12 weeks	16 weeks
Ct.V (mm^3)	$0.53 \pm 0.07^{s,a}$	0.77 ± 0.05^{a}	0.84 ± 0.10^{s}	0.81 ± 0.13
Ct.V/TV (%)	$51.80 \pm 5.99^{s,a}$	$66.93 \pm 3.56^{s,a}$	$85.07 \pm 1.75^{s,a}$	$88.27 \pm 1.57^{s,a}$
Ct.Th (mm)	$0.18 \pm 0.01^{s,a}$	$0.24 \pm 0.02^{s,a}$	$0.32 \pm 0.02^{s,a}$	$0.35 \pm 0.03^{s,a}$
T.Ar (mm^2)	$0.43 \pm 0.06^{s,a}$	$0.58 \pm 0.03^{s,a}$	0.70 ± 0.06^{s}	0.66 ± 0.06^{s}
F_u (N)	$10.4 \pm 1.6^{s,a}$	16 ± 1.7^{a}	16.9 ± 20^{s}	16.9 ± 3.0
S (N/mm)	$38.5 \pm 8.7^{s,a}$	$51.2 \pm 6.9^{s,a}$	$57.3 \pm 17.5^{s,a}$	$89.7 \pm 9.2^{s,a}$
d (mm)	0.28 ± 0.06	0.29 ± 0.03^{s}	0.30 ± 0.07^{a}	0.20 ± 0.05^{a}
U (N/mm)	1.7 ± 0.5^{s}	2.7 ± 0.6^{a}	$3.0 \pm 0.8^{s,a}$	2.0 ± 0.7^{a}

Data presented as mean ± SD. [s] Strain significantly different, [a] Age significantly different (one-way ANOVA, post hoc LSD, $P < 0.01$)

Morphometry: Ct.V, neck cortical bone volume; Ct.V/TV, neck cortical bone volume density; Ct.Th, neck cortical thickness; T.Ar, neck average cross-sectional area. Mechanics: F_u, strength; S, stiffness; d, deformation to failure; U, work to failure

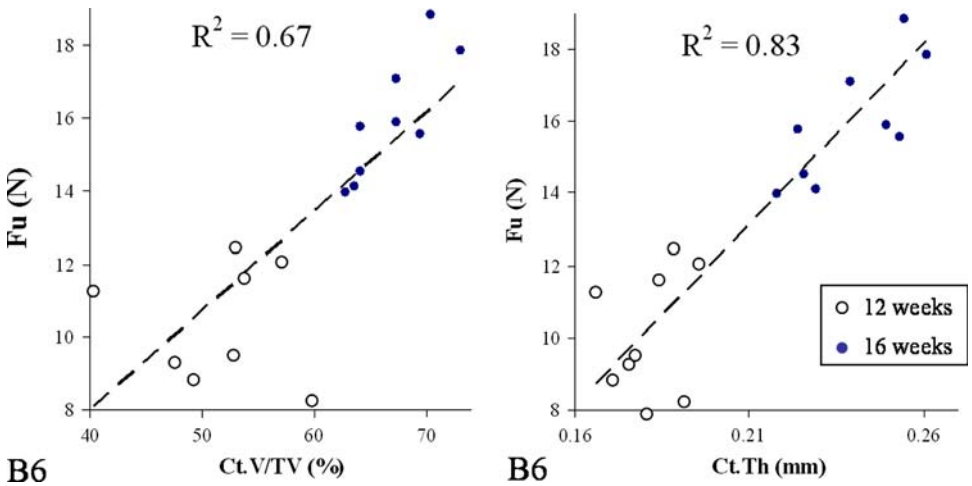

Fig. 4 Femoral neck morphometric parameters (*left* Ct.V/TV, $R^2 = 0.67$; *right* Ct.Th, $R^2 = 0.83$) showed a good correlation with femoral strength in B6 inbred strain of mice

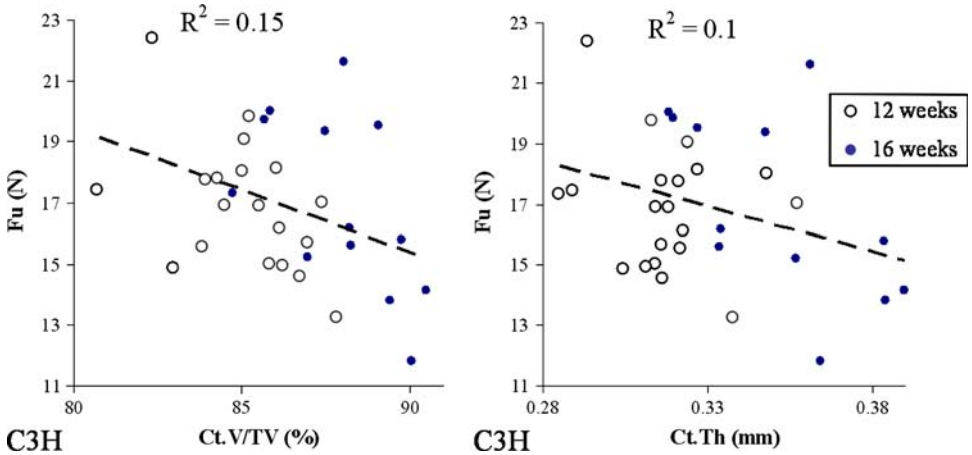

Fig. 5 Femoral neck morphometric parameters (*left* Ct.V/TV, $R^2 = 0.15$; *right* Ct.Th, $R^2 = 0.1$) did not correlate well with femoral strength in C3H inbred strain of mice

In order to even better predict B6 strength from structural parameters, multiple linear regression analyses including morphometric indices of compartments I (full bone), III (midshaft cortical bone), and IV (neck cortical bone) were also computed. Adding full AVD and diaphysis Ct.Th to neck Ct.Th could not better explain B6 strength than neck Ct.Th alone. In C3H, multiple linear regression analyses including different compartments only slightly improved the predictive power of morphometry on mechanics, but correlations did not reach significance.

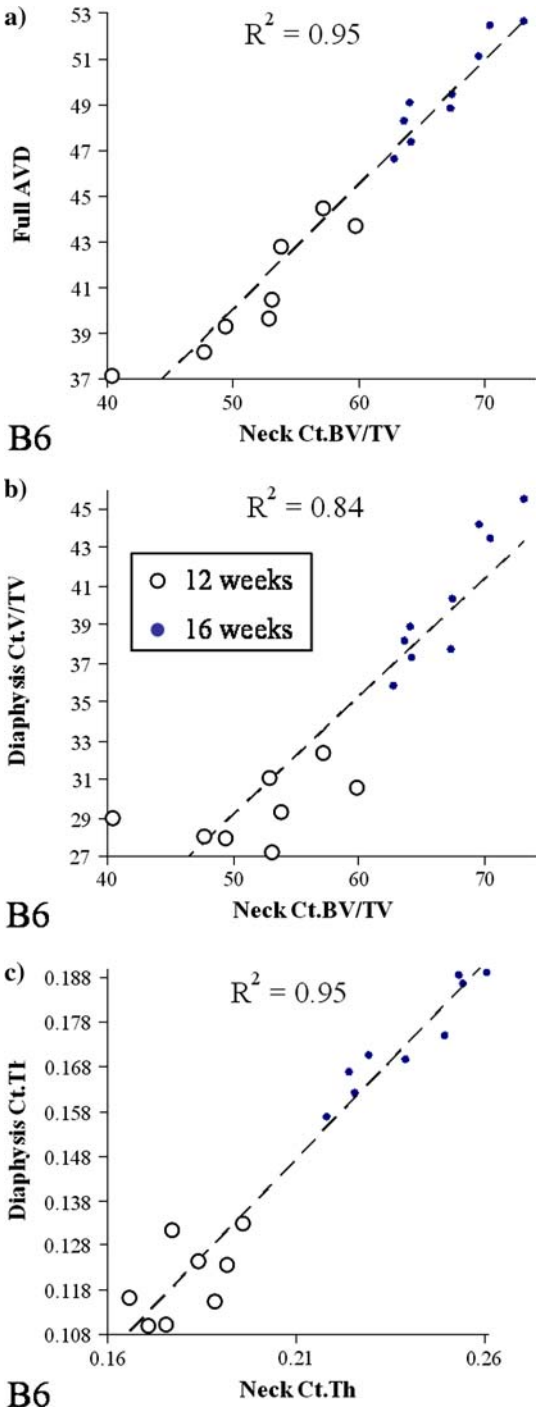

Fig. 6 Correlation of cortical bone volume density in the femoral neck with full bone apparent volume density (**a**) and diaphyseal cortical bone volume density (**b**). Correlation of femoral neck cortical thickness with diaphyseal cortical thickness (**c**)

Discussion

In this study, mechanical tests of B6 and C3H inbred strains of mice were performed by axial loading of the femoral head. Our tests revealed that B6 femora became stiffer, stronger, and tougher at 12–16 weeks, whereas bone brittleness stayed constant. C3H behaved differently in this time period: Stiffness increased but strength remained constant, work to failure decreased, and bone became more brittle. We used μCT to assess structural bone parameters, including those at the femoral neck, which to our knowledge has not been done before. Our results showed that 83% of mechanical strength of the femoral neck in the B6 strain was explained by the cortical thickness at this location; in contrast, none of the mechanical properties was explained by bone morphometry in the C3H strain.

The different evolutions of mechanical properties in the two strains with aging confirmed previous studies showing that B6 mice do not reach material and mechanical peak bone properties before 20 weeks [39, 40]. Indeed, bone mechanical properties, such as strength, stiffness, and work to failure, increased between 12 and 16 weeks. On the other hand, our results for C3H suggested that maximal skeletal biomechanical properties were already reached before 16 weeks since strength stayed constant, bone became more brittle, and work to failure decreased. The increase in brittleness and the reduction of work to failure are typical characteristics of bone aging after reaching maximal skeletal biomechanical properties [41–43]. Bone is a natural composite, comprising mineral (mainly hydroxyapatite), organic (mostly type I collagen), and water phases [44]. Jepsen [42] reported that changes of the bone matrix were associated with aging. The aging bone becomes more porous and locally more highly mineralized and accumulates more microdamage. These changes are central to the evolution of bone brittleness. Similarly, Wang et al. [43] showed that the mechanical integrity of the collagen network deteriorates with increasing age and correlates significantly with the decreased work to failure of aged bone.

In the B6 strain, strength was the only bone mechanical parameter that was significantly influenced by bone geometry and microstructure. Considering that failure always occurred in the femoral neck, the neck apparently is the weakest part of the bone, at least in this specific loading configuration. Hence, it is not surprising that bone strength only depended on material and geometric properties intrinsic to the femoral neck. The other parameters—stiffness, brittleness, and toughness—are dependent on the deformation of the entire bone. Because it is not only the neck but also the femoral diaphysis that deformed during the compression tests, these mechanical parameters rely on a more complicated deformation process, including compression, bending, and shear in the whole bone. In order to take more structural properties into account, other compartments in the mid-diaphysis and the distal metaphysis as well as the full bone (compartments I, II, and III) were

investigated; however, they did not increase the predictive power.

This study showed that the cortical compartments were better predictors than the trabecular ones. Bone strength in the femoral neck of B6 was mainly determined by cortical bone density and cortical thickness. The neck trabecular compartment showed only little bone and a low number of trabeculae. Murine proximal femur contains proportionally thicker cortical bone and a less dense trabecular network than in humans [45]. In the neck trabecular compartment, we saw that the trabecular network was concentrated on both ends of the neck, close to the shaft and to the head (Fig. 1). However, the neck fractures occurred mostly in the middle of the neck, where no trabecular bone was present. At this location, strength was determined only by cortical bone properties. Cortical neck morphometric parameters explained bone strength in B6 but not in C3H. C3H morphometric properties in particular varied much less with age than those of B6, which was one of the reasons that correlations between morphometry and strength were lower in C3H than in B6 (Table 1, Figs. 4 and 5). Since the two strains showed similar variation in strength, this implies that strength in C3H bone, much more than in B6, is determined not only by structural but also by other bone properties, often referred to as "bone quality" [46–48]. The term "bone quality" incorporates the effects of ultrastructural properties such as mineralization, microporosity, microdamage, the distribution and activity of the three main cell types in bone (osteoclasts, osteoblasts, and osteocytes), and collagen quality. Biomechanics of the bone tissue will not be fully understood as long as these parameters' contribution to and interaction with bone strength will not be completely identified, analyzed, and quantified. There are already a number of studies that have investigated different contributions to bone strength [33]. Highly mineralized bone is stiffer, more brittle, and less tough than bone with less mineralization [42, 49]. The increase of overall porosity in cortical bone is also responsible for a decrease of bone mechanical properties [50, 51], whereas the quality of the collagen matrix was shown to predominantly determine the work to failure of bone [43, 52–55]. Further, it was reported that bone cells had different levels of activity in various inbred strains, resulting in different bone tissue properties, especially in the amount of minerals and remodeling rates [56, 57]. Finally, microdamage accumulation is central to the strength, work to failure, brittleness, and fatigue resistance of bone. For a composite material like bone, failure is the end result of a damage accumulation process [42, 58, 59]. The high brittleness of C3H compared to B6 can be explained, to some extent, by higher BMD [60] but also suggests that C3H bone is more porous and accumulates more microdamage. Investigation of cortical porosity and microdamage initiation and propagation in mouse inbred strains may help to uncover the processes at the ultrastructural level which lead to bone failure and, consequently, may further improve our understanding of bone failure behavior.

Before concluding, we would like to discuss the reasons for working with groups of different ages. If limited to a single age group, the regressions between morphometry and mechanics would be much less robust. Indeed, a population of the same strain is made of very similar individuals. The variability in morphometric indices would then be very small. Thus, with small variations, strong regression would be very difficult to achieve. In fact, due to the small variations within an inbred strain, any possible relationships between bone morphometry and bone strength at a particular age might be obscured by small experimental errors. It is only by combining age groups that a more diverse population is created which allows detection of such relationships. Populations of different ages increase the variations and therefore emphasize the contribution of morphometry to the mechanical parameters of bone. The relationships per age group nicely match up with the overall picture, further providing evidence that the age groups can be combined. In addition, only morphometric parameters had smaller variations in C3H than in B6, while mechanical parameters did not. In fact, mechanical parameters varied in the same ranges in both strains. This last observation led us to the conclusion that morphometry is a poorer indicator in C3H. Finally, we chose different age groups also because we wanted to investigate the influence of age on mechanical and morphometric parameters and show the differences in C3H and B6.

This study demonstrated differences in mechanical properties of the femoral neck under axial loading between the two inbred strains B6 and C3H. Bone strength in B6 was explained, to a great extent, by the cortical thickness at the femoral neck, while in C3H no morphometric parameter could predict it. We conclude that the relative contributions of bone structural and material properties to bone strength are different in B6 and C3H. We hypothesize that these different contributions are related to differences at the ultrastructural level of bone that affect bone failure.

Acknowledgements This work was supported through ETH Intramural Funding (TH 00124/41-2631.5) and the Swiss National Science Foundation (FP 620-58097.99, PP-104317/1). We thank Paul Lüthi for indispensable help with our loading device.

References

1. WHO (1999) Osteoporosis: both health organizations and individuals must act now to avoid an impending epidemic. Press Release WHO/58. http://www.who.int/inf-pr-1999/en/pr99-58.html

2. Chevalley T, Rizzoli R, Nydegger V, Slosman D, Tkatch L, Rapin CH, Vasey H, Bonjour JP (1991) Preferential low bone mineral density of the femoral neck in patients with a recent fracture of the proximal femur. Osteoporos Int 1:147–154
3. Cummings SR, Nevitt MC, Browner WS, Stone K, Fox KM, Ensrud KE, Cauley J, Black D, Vogt TM (1995) Risk factors for hip fracture in white women. Study of Osteoporotic Fractures Research Group. N Engl J Med 332:767–773
4. Duboeuf F, Hans D, Schott AM, Kotzki PO, Favier F, Marcelli C, Meunier PJ, Delmas PD (1997) Different morphometric and densitometric parameters predict cervical and trochanteric hip fracture: the EPIDOS Study. J Bone Miner Res 12:1895–1902
5. Faulkner KG, Cummings SR, Nevitt MC, Pressman A, Jergas M, Genant HK (1995) Hip axis length and osteoporotic fractures. Study of Osteoporotic Fractures Research Group. J Bone Miner Res 10:506–508
6. Gnudi S, Ripamonti C, Gualtieri G, Malavolta N (1999) Geometry of proximal femur in the prediction of hip fracture in osteoporotic women. Br J Radiol 72:729–733
7. Cummings SR, Cauley JA, Palermo L, Ross PD, Wasnich RD, Black D, Faulkner KG (1994) Racial differences in hip axis lengths might explain racial differences in rates of hip fracture. Study of Osteoporotic Fractures Research Group. Osteoporos Int 4:226–229
8. Faulkner KG, Cummings SR, Black D, Palermo L, Gluer CC, Genant HK (1993) Simple measurement of femoral geometry predicts hip fracture: the study of osteoporotic fractures. J Bone Miner Res 8:1211–1217
9. Silver L (1995) Mouse genetics. Oxford University Press, New York
10. Peng Z, Tuukkanen J, Zhang H, Jamsa T, Vaananen HK (1994) The mechanical strength of bone in different rat models of experimental osteoporosis. Bone 15:523–532
11. Sogaard CH, Danielsen CC, Thorling EB, Mosekilde L (1994) Long-term exercise of young and adult female rats: effect on femoral neck biomechanical competence and bone structure. J Bone Miner Res 9:409–416
12. Turner CH, Hsieh YF, Müller R, Bouxsein ML, Rosen CJ, McCrann ME, Donahue LR, Beamer WG (2001) Variation in bone biomechanical properties, microstructure, and density in BXH recombinant inbred mice. J Bone Miner Res 16:206–213
13. Turner CH, Sun Q, Schriefer J, Pitner N, Price R, Bouxsein ML, Rosen CJ, Donahue LR, Shultz KL, Beamer WG (2003) Congenic mice reveal sex-specific genetic regulation of femoral structure and strength. Calcif Tissue Int 73:297–303
14. Turner CH, Takano Y, Hirano T (1996) Reductions in bone strength after fluoride treatment are not reflected in tissue-level acoustic measurements. Bone 19:603–607
15. Tuukkanen J, Peng Z, Vaananen HK (1994) Effect of running exercise on the bone loss induced by orchidectomy in the rat. Calcif Tissue Int 55:33–37
16. Borah B, Dufresne TE, Chmielewski PA, Johnson TD, Chines A, Manhart MD (2004) Risedronate preserves bone architecture in postmenopausal women with osteoporosis as measured by three-dimensional microcomputed tomography. Bone 34:736–746
17. Eckstein F, Lochmuller EM, Koller B, Wehr U, Weusten A, Rambeck W, Hoeflich A, Wolf E (2002) Body composition, bone mass and microstructural analysis in GH-transgenic mice reveals that skeletal changes are specific to bone compartment and gender. Growth Horm IGF Res 12:116–125
18. Ito M, Nishida A, Nakamura T, Uetani M, Hayashi K (2002) Differences of three-dimensional trabecular microstructure in osteopenic rat models caused by ovariectomy and neurectomy. Bone 30:594–598
19. Müller R (2003) Bone microarchitecture assessment: current and future trends. Osteoporos Int 14(Suppl 5):89–99
20. Müller R, Rüegsegger P (1997) Micro-tomographic imaging for the nondestructive evaluation of trabecular bone architecture. Stud Health Technol Inform 40:61–79
21. Rüegsegger P, Koller B, Muller R (1996) A microtomographic system for the nondestructive evaluation of bone architecture. Calcif Tissue Int 58:24–29
22. Alexander JM, Bab I, Fish S, Müller R, Uchiyama T, Gronowicz G, Nahounou M, Zhao Q, White DW, Chorev M, Gazit D, Rosenblatt M (2001) Human parathyroid hormone 1–34 reverses bone loss in ovariectomized mice. J Bone Miner Res 16:1665–1673
23. Balto K, Müller R, Carrington DC, Dobeck J, Stashenko P (2000) Quantification of periapical bone destruction in mice by micro-computed tomography. J Dent Res 79:35–40
24. Kapadia RD, Stroup GB, Badger AM, Koller B, Levin JM, Coatney RW, Dodds RA, Liang X, Lark MW, Gowen M (1998) Applications of micro-CT and MR microscopy to study pre-clinical models of osteoporosis and osteoarthritis. Technol Health Care 6:361–372
25. Müller R, Van Campenhout H, Van Damme B, Van Der Perre G, Dequeker J, Hildebrand T, Rüegsegger P (1998) Morphometric analysis of human bone biopsies: a quantitative structural comparison of histological sections and micro-computed tomography. Bone 23:59–66
26. Schmidt K, Schinke T, Haberland M, Priemel M, Schilling AF, Mueldner C, Rueger JM, Sock E, Wegner M, Amling M (2005) The high mobility group transcription factor Sox8 is a negative regulator of osteoblast differentiation. J Cell Biol 168:899–910
27. Jepsen KJ, Akkus OJ, Majeska RJ, Nadeau JH (2003) Hierarchical relationship between bone traits and mechanical properties in inbred mice. Mamm Genome 14:97–104
28. Tommasini SM, Morgan TG, van der Meulen M, Jepsen KJ (2005) Genetic variation in structure–function relationships for the inbred mouse lumbar vertebral body. J Bone Miner Res 20:817–827
29. Turner CH, Hsieh YF, Müller R, Bouxsein ML, Baylink DJ, Rosen CJ, Grynpas MD, Donahue LR, Beamer WG (2000) Genetic regulation of cortical and trabecular bone strength and microstructure in inbred strains of mice. J Bone Miner Res 15:1126–1131
30. Akhter MP, Cullen DM, Pedersen EA, Kimmel DB, Recker RR (1998) Bone response to in vivo mechanical loading in two breeds of mice. Calcif Tissue Int 63:442–449
31. Kodama Y, Umemura Y, Nagasawa S, Beamer WG, Donahue LR, Rosen CR, Baylink DJ, Farley JR (2000) Exercise and mechanical loading increase periosteal bone formation and whole bone strength in C57BL/6J mice but not in C3H/Hej mice. Calcif Tissue Int 66:298–306
32. Beamer WG, Sen S, Churchill GA, Rosen CJ, Donahue LR, Shultz KL, Mytar J, Turner CH, Müller R, Uchiyama T, Bouxsein ML (2001) Genetic relationships among bone phenotypes regulated by sets of quantitative trait loci (QTL) in B6C3F2 mice. J Bone Miner Res 16:S197
33. Ng AH, Wang SX, Turner CH, Beamer WG, Grynpas MD (2007) Bone quality and bone strength in BXH recombinant inbred mice. Calcif Tissue Int 81:215–223
34. Kohler T, Beyeler M, Webster D, Müller R (2005) Compartmental bone morphometry in the mouse femur: reproducibility and resolution dependence of microtomographic measurements. Calcif Tissue Int 77:281–290
35. Hildebrand T, Rüegsegger P (1997) A new method for the model-independent assessment of thickness in three-dimensional images. J Microsc 185:67–75
36. Rüegsegger P, Koller B, Müller R (1996) A microtomographic system for the nondestructive evaluation of bone architecture. Calcif Tissue Int 58:24–29

37. Hildebrand T, Laib A, Müller R, Dequeker J, Rüegsegger P (1999) Direct three-dimensional morphometric analysis of human cancellous bone: microstructural data from spine, femur, iliac crest, and calcaneus. J Bone Miner Res 14:1167–1174
38. Voide R, van Lenthe GH, Müller R (2008) Femoral stiffness and strength critically depend on loading angle—a parametric study in a mouse inbred strain. Biomed Tech. doi: 10.1515/BMT.2008.019
39. Brodt MD, Ellis CB, Silva MJ (1999) Growing C57Bl/6 mice increase whole bone mechanical properties by increasing geometric and material properties. J Bone Miner Res 14:2159–2166
40. Ferguson VL, Ayers RA, Bateman TA, Simske SJ (2003) Bone development and age-related bone loss in male C57BL/6J mice. Bone 33:387–398
41. Boivin G, Meunier PJ (2003) The mineralization of bone tissue: a forgotten dimension in osteoporosis research. Osteoporos Int 14(Suppl 3):S19–S24
42. Jepsen KJ (2003) The aging cortex: to crack or not to crack. Osteoporos Int 14(Suppl 5):57–66
43. Wang X, Shen X, Li X, Agrawal CM (2002) Age-related changes in the collagen network and toughness of bone. Bone 31:1–7
44. Katz JL (1971) Hard tissue as a composite material. I. Bounds on the elastic behavior. J Biomech 4:455–473
45. Jamsa T, Tuukkanen J, Jalovaara P (1998) Femoral neck strength of mouse in two loading configurations: method evaluation and fracture characteristics. J Biomech 31:723–729
46. Cooper C (1993) The epidemiology of fragility fractures: is there a role for bone quality? Calcif Tissue Int 53(Suppl 1):S23–S26
47. Schnitzler CM (1993) Bone quality: a determinant for certain risk factors for bone fragility. Calcif Tissue Int 53(Suppl 1):S27–S31
48. Wallach S, Feinblatt JD, Carstens JH Jr, Avioli LV (1992) The bone "quality" problem. Calcif Tissue Int 51:169–172
49. Simmons ED Jr, Pritzker KP, Grynpas MD (1991) Age-related changes in the human femoral cortex. J Orthop Res 9:155–167
50. Evans F (1976) Changes in mechanical properties and histology of human compact bone. Colombus
51. Currey JD (1988) The effect of porosity and mineral content on the Young's modulus of elasticity of compact bone. J Biomech 21:131–139
52. Boskey AL, Wright TM, Blank RD (1999) Collagen and bone strength. J Bone Miner Res 14:330–335
53. Burstein AH, Zika JM, Heiple KG, Klein L (1975) Contribution of collagen and mineral to the elastic-plastic properties of bone. J Bone Joint Surg Am 57:956–961
54. Currey JD, Foreman J, Laketic I, Mitchell J, Pegg DE, Reilly GC (1997) Effects of ionizing radiation on the mechanical properties of human bone. J Orthop Res 15:111–117
55. Zioupos P, Currey JD, Hamer AJ (1999) The role of collagen in the declining mechanical properties of aging human cortical bone. J Biomed Mater Res 45:108–116
56. Sheng MH, Baylink DJ, Beamer WG, Donahue LR, Rosen CJ, Lau KH, Wergedal JE (1999) Histomorphometric studies show that bone formation and bone mineral apposition rates are greater in C3H/HeJ (high-density) than C57BL/6J (low-density) mice during growth. Bone 25:421–429
57. Sheng MH, Lau KH, Beamer WG, Baylink DJ, Wergedal JE (2004) In vivo and in vitro evidence that the high osteoblastic activity in C3H/HeJ mice compared to C57BL/6J mice is intrinsic to bone cells. Bone 35:711–719
58. Jepsen KJ, Schaffler MB, Kuhn JL, Goulet RW, Bonadio J, Goldstein SA (1997) Type I collagen mutation alters the strength and fatigue behavior of Mov13 cortical tissue. J Biomech 30:1141–1147
59. Schaffler MB, Choi K, Milgrom C (1995) Aging and matrix microdamage accumulation in human compact bone. Bone 17:521–525
60. Wergedal JE, Sheng MH, Ackert-Bicknell CL, Beamer WG, Baylink DJ (2005) Genetic variation in femur extrinsic strength in 29 different inbred strains of mice is dependent on variations in femur cross-sectional geometry and bone density. Bone 36:111–122